Journal of Applied Electrochemistry (2005) 35:945–953
DOI 10.1007/s10800-005-7078-2

Electro-oxidation of carbonate in aqueous solution on a platinum rotating ring disk electrode

JIUJUN ZHANG[1,*] and COLIN W. OLOMAN[2]
[1]*Institute for Fuel Cell Innovation, National Research Council Canada, Vancouver, B.C., V67 1W5, Canada*
[2]*Department of Chemical and Biological Engineering and Pulp & Paper Centre, University of British Columbia, Vancouver, B.C., Canada V6T 1Z4,*
*(*author for correspondence, tel.: +1-604221-3087, fax: +1-604-221-3001, e-mail: jiujun.zhang@nrc.gc.ca)*

Received 28 August 2004; accepted in revised form 13 April 2005

Key words: carbonate, electro-oxidation, electro-synthesis, hydrogen peroxide, kinetics, percarbonate, platinum, rotating ring-disk electrode

Abstract

The kinetics of electro-oxidation of carbonate aqueous solution on a platinum electrode were examined by a rotating ring (platinum) – disk (platinum) electrode in aqueous sodium carbonate/bicarbonate solutions (25 °C, pH = 10.75) with the peroxide stabilizing additives sodium silicate, magnesium sulphate and sodium DTPA such as are used in brightening mechanical wood pulp. A theoretical model based on the experimental data is proposed to describe this electro-oxidation process. The model shows consistency between the experimental results and the expectation from the proposed reaction sequence. The first-order rate constants at 25 °C, pH = 10.75 in 1.13 M (Na_2CO_3 + $NaHCO_3$) for carbonate electro-oxidation to percarbonate (a.k.a. peroxidicarbonate $C_2O_6^{2-}$), percarbonate hydrolysis to hydrogen peroxide and hydrogen peroxide electro-oxidation to oxygen are estimated from the experimental data, respectively, as $(1.43 \pm 0.1) \times 10^{-11}$cm s^{-1} (extrapolated to the equilibrium electrode potential which is estimated as ca. 0.21 (vs SCE)), $(1.1 \pm 0.2) \times 10^{-2}$ s^{-1} and $(5.6 \pm 0.5) \times 10^{-8}$cm s^{-1} (extrapolated to the equilibrium electrode potential of −0.019 V (vs SCE)).

Nomenclature

$(CE)_{anode}$	anode current efficiency for percarbonate ($=(I_D - I_B)/I_D$)
C_{CO_3}	total concentration of carbonate (mol dm^{-3})
$D^{2-}_{C_2O_6}$	diffusion coefficient for $C_2O_6^{2-}$ (cm^2 s^{-1})
$D_{H_2O_2}$	diffusion coefficient for H_2O_2 (cm^2 s^{-1})
E	electrode potential (V (vs SCE))
$E^{o(C_2O_6/CO_3)}$	equilibrium electrode potential for reaction 1 (V (vs. SCE))
$E^{o(H_2O_2/O_2)}$	equilibrium electrode potential for reaction III (V (vs SCE))
$E^{o(O_2/H_2O)}$	equilibrium electrode potential for reaction V (V (vs SCE))
F	Faraday's number (96480 C mol^{-1})
I_B	background current (mA)
I_D	disk current (mA)
I'_D	net disk current ($=I_D - I_B$) (mA)
I_R	ring current (mA)
k_1	potential-dependent rate constant for reaction (VIII) (cm s^{-1})
k_2	potential-dependent rate constant for reaction (XII) (cm s^{-1})
k_1°	standard rate constant at equilibrium electrode potential $E^{o(C_2O_3/CO_3)}$ for redox couple $CO_3^{2-}/C_2O_6^{2-}$ (cm s^{-1})
k_2°	standard rate constant at equilibrium electrode potential $E^{o(H_2O_2/O_2)}$ for redox couple H_2O_2/O_2 (cm s^{-1})
K_{a1}	first acidic dissociation constant for H_2CO_3 (mol dm^{-3})
K_{a2}	secondary acidic dissociation constant for H_2CO_3 (mol dm^{-3})
k_d	decomposition rate constant for reaction (XIII) (cm s^{-1})
k_h	hydrolysis rate constant for reaction (IX) (cm s^{-1})
k_{db}	bulk solution decomposition rate constant for reaction (XV) (s^{-1})
k_{hb}	bulk solution hydrolysis rate constant for reaction (XI) (s^{-1})
n_1	electrochemical stoichiometry coefficient for carbonate electro-oxidation ($=2$)
n_2	electrochemical stoichiometry coefficient for hydrogen oxidation ($=2$)

$n_{\alpha 1}$ controlling-step electron transfer number for carbonate electro-oxidation (assumed = 1)

$n_{\alpha 2}$ controlling-step electron transfer number for hydrogen peroxide electro-oxidation (assumed = 1)

N° standard ring electrode collection efficiency

r_1 diffusion rate constant for equation (X) ($= 0.201(D^{2-}_{C_2O_6})^{2/3}\nu^{-1/6}$, cm $s^{-1/2}$)

r_2 diffusion rate constant for equation (XIV) ($= 0.201\,(D_{H_2O_2})^{2/3}\ \nu^{-1/6}$, cm $s^{-1/2}$)

R gas constant (8.314 J K^{-1} mol^{-1})

T temperature (K)

w_1 diffusion layer constant for $C_2O_6^{2-} = 4.98(D_{C_2O_6})^{1/3}\nu^{1/6}$, cm $s^{-1/2}$)

w_2 diffusion layer constant for H_2O_2 ($= 4.98(D_{H_2O_2})^{1/3}\nu^{1/6}$, cm $s^{-1/2}$)

α_1 electron transfer coefficient for carbonate electro-oxidation

α_2 electron transfer coefficient for peroxide electro-oxidation

ω electrode rotation rate (rpm)

ν kinematic viscosity of aqueous solution (0.012 cm^2 s^{-1})

1. Introduction

The electrochemical oxidation of carbonate in aqueous solution on a platinum electrode has been employed by previous workers to synthesize oxidizing bleaching solutions derived from percarbonate ($C_2O_6^{2-}$, also called electroytic percarbonate, peroxydicarbonate, peroxocarbonate or peroxycarbonate) [1–3]. Fundamental studies on this electro-oxidation process have been carried out over many years by various methods such as polarographic, steady polarization, electrolysis, isotope-exchange, chemical titration, and rotating electrode techniques [1–20].

It has been shown that there are two kinds of "percarbonate", one is the electrolytic percarbonate and the other is the chemical percarbonate. The electrolytic percarbonate is a true percarbonate produced by anode oxidation of cold (e.g. −10 °C) carbonate solution on a noble metal electrode such as platinum [1–20] to give a sodium (or potassium) salt with the proposed formula $Na_2C_2O_6$, and the corresponding chemical structure shown in Figure 1(a) [21–23]. The chemical sodium (or potassium) "percarbonate" is a commercial product obtained by simply mixing H_2O_2 and Na_2CO_3 in an alkaline solution. The chemical percarbonate salt, written as $2Na_2CO_3{\cdot}3H_2O_2$, is considered to be a hydrogen bonded adduct between H_2O_2 and Na_2CO_3 with a chemical structure as shown in Figure 1(b) [24, 25].

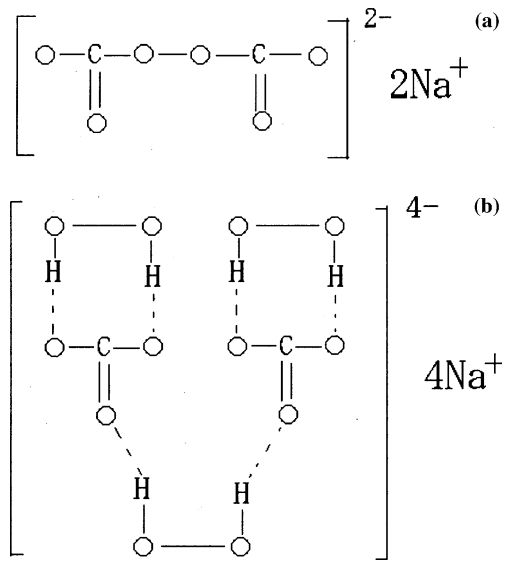

Fig. 1. Proposed structures for sodium percarbonate [21–23]: (a) Electrolytic percarbonate, (b) Chemical percarbonate [24–25].

It has been recognized from chemical and electrochemical measurements that the percarbonate ion produced by electro-oxidation of carbonate in aqueous solution (Reaction I) is hydrolysed to peroxide according to reaction II, in a pseudo-first order reaction with excess solvent and a half-life estimated as 1–2 min at 15 °C, pH 10 [7, 12, 13].

$$C_2O_6^{2-} + 2e^- \leftrightarrow 2CO_3^{2-} \quad E^{o(C_2O_6/CO_3)}\text{ca. } 0.21\ \text{V (vs SCE) at } 25\,^\circ\text{C, pH } 10.75\text{[7]} \qquad \text{(I)}$$

$$C_2O_6^{2-} + 2H_2O \leftrightarrow H_2O_2 + 2HCO_3^- \qquad \text{(II)}$$

The peroxide from reaction II can be further oxidized on the electrode (reaction III) in the potential range of carbonate oxidation or can disproportionate to water (reaction IV), thus decreasing the current efficiency for active oxygen generation [12, 13]:

$$O_2 + 2H^+ + 2e^- \leftrightarrow H_2O_2 \quad E^{o(H_2O_2/O_2)} = -0.19\,\text{V (vs SCE) at } 25\,^\circ\text{C, pH } 10.75\ [32] \qquad \text{(III)}$$

$$H_2O_2 \rightarrow 1/2O_2 + H_2O \qquad \text{(IV)}$$

On the other hand, the parasitic oxidation of solvent H_2O (reaction V) also reduces the current efficiency for percarbonate formation:

$$O_2 + 4H^+ + 4e^- \leftrightarrow 2H_2O \quad E^{o(O_2/H_2O)} = 0.35\text{V(vs SCE) at } 25\,^\circ\text{C, pH } 10.75\ [32] \qquad \text{(V)}$$

The electrochemical/chemical processes of carbonate oxidation are complicated and, although some pioneering information has been reported [1–20], the mechanism and kinetics of this process have not been well-explored. The detailed molecular level reaction mechanism should involve processes such as the electrode surface adsorption and the formation of short-lived intermediates or radicals. However, due to the limitations of our objective and the capability of

instrumental analysis in our facility, the reaction mechanism for carbonate electro-oxidation at such detail level will not be examined in this paper. The work described in this paper, done at the U.B.C. Pulp and Paper Centre, was aimed at the development of a quantitative kinetic model and measurement method for the electro-oxidation of carbonate to support our work on *in-situ* brightening of mechanical pulp by electrolysis of sodium carbonate solutions [3].

A rotating ring (platinum) – disk (platinum) electrode was employed in this work to obtain the electrochemical data for carbonate oxidation, based on which a kinetic model was developed according to a proposed reaction sequence. The agreement between the experimental results and theoretical expectation allows the estimation of rate constants of the electro-oxidation of carbonate to percarbonate, the hydrolysis of percarbonate to hydrogen peroxide, and the further oxidation and/or disproportionation of H_2O_2 to O_2

2. Experimental

2.1. *Chemicals and solutions*

The reagent-grade sodium carbonate (Na_2CO_3), sodium bicarbonate ($NaHCO_3$), hydrogen peroxide (H_2O_2, 30% in water), sodium silicate ($Na_2SO_3{\cdot}5H_2O$), magnesium sulfate ($MgSO_4{\cdot}7H_2O$), and sodium Perchlorate ($NaClO_4$) were purchased from Fisher Scientific and used without further purification. Diethylenetriaminepentaacetic acid, sodium salt (40% in water, abbreviated as DTPA, Acros Organics) was used as received. Water which was used to prepare the solutions was purified by double distillation with $KMnO_4$. The pH of the solution was controlled with the $Na_2CO_3/NaHCO_3$ ratio. In the experiments determining the effect of supporting electrolyte, 0.1–1.0 mol dm^{-3} $NaClO_4$ was added to the testing solutions as a supporting electrolyte. In the test solutions, 0.03 mol dm^{-3} Na_2SiO_3 + 8×10^{-5} mol dm^{-3} DTPA + 3×10^{-4} mol dm^{-3} $MgSO_4$ were added for peroxide stabilizing and for simulating the real situation of a wood pulp brightening liquor. Solutions were de-aerated prior to the tests by sparging with argon gas (99.9 % vol).

2.2. *Electrode preparation*

A ring (platinum) – disk (platinum) electrode purchased from Pine Instruments was used as received. The electrode was polished using 0.3 μm alumina powder, sonicated for 5 min in water and rinsed with acetone and water before each experiment. The disk electrode area, 0.16 cm^2, and the ring electrode collection efficiency (N°), 0.223, were calibrated using a solution of 0.01 mol dm^{-3} $[Fe(CN)_6]^{3-}$. The counter electrode was a platinum wire, and a saturated calomel electrode (SCE) was employed as reference electrode. All potentials reported in this paper are quoted with respect to the SCE.

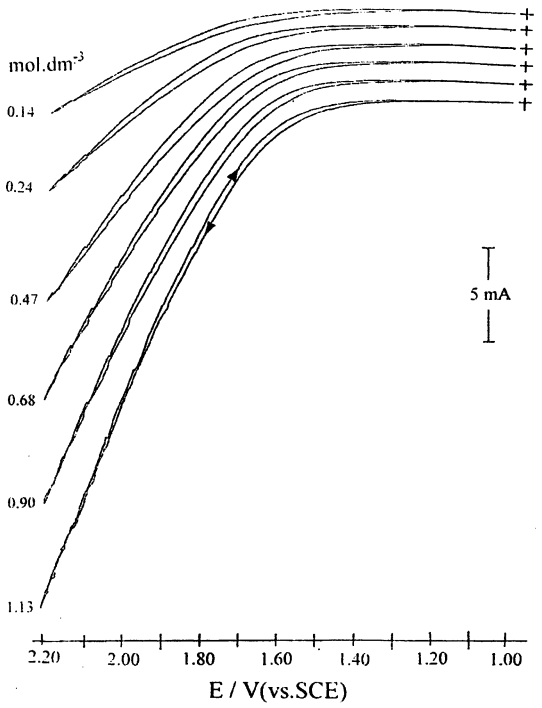

Fig. 2. Electro-oxidation of carbonate on a rotating platinum disk electrode (3600 rpm) in a solution (0.03 mol dm^{-3} Na_2SiO_3 + 8×10^{-5} mol dm^{-3} DTPA + 3×10^{-4} mol dm^{-3} $MgSO_4$, pH 10.75) containing various concentrations of sodium carbonate + sodium bicarbonate as marked at left-side of the curves. Potential scan rate: 20 mV s^{-1}. The potential is for disk electrode.

2.3. *Apparatus and procedures*

A conventional three-compartment cell was used to perform the electrochemical measurements. An RDE3 potentiostat, a MSRX rotator (Pine Instruments), and an X–Y recorder were employed to record the current–potential data.

All experiments were carried out at ambient laboratory temperature (25 ± 2 °C) and pressure (1 atm absolute).

3. Results and discussion

3.1. *Experiment results*

Figure 2 shows the current–potential curves for solutions with various concentrations of carbonate/bicarbonate, containing the pulp brightening (a.k.a. peroxide stabilizing) additives Na_2SiO_3, $MgSO_4$, and DTPA, recorded on a platinum disk electrode rotated at 3600 rpm, The marked number on the left side of each curve in Figure 2 is the total concentration of carbonate and bicarbonate (defined as C_{CO_3}, i.e, $C_{CO_3} = [CO_3^{2-}] + [HCO_3^-] + [H_2CO_3]$). For a solution at high pH such as 10.75, the concentration of H_2CO_3 is negligible, therefore, C_{CO_3} is actually the sum of $[CO_3^{2-}] + [HCO_3^-]$. The solution pH in each concentration was adjusted to 10.75 by adding an extra small amount of 1.0 mol dm^{-3} Na_2CO_3 or $NaHCO_3$. It was found that the ionic migration effect [26] in these solutions could be neglected because the

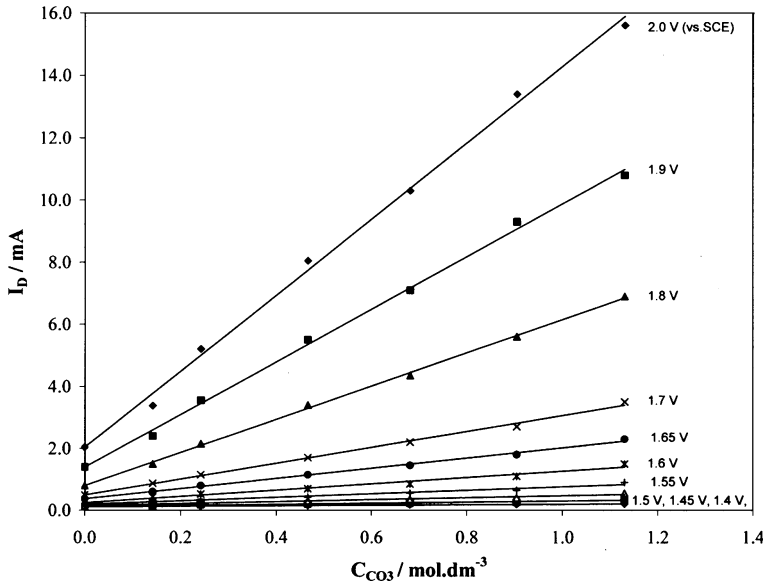

Fig. 3. Plots of disk current in Figure 2 vs the concentration of carbonate at various disk electrode potentials as marked at the right-side of the plots.

data of Figure 2 were not affected by adding 0.1–1.0 mol dm^{-3} $NaClO_4$ supporting electrolyte. The increase in the oxidation current with carbonate concentration clearly indicates the occurrence of carbonate electro-oxidation (reaction I). A background current–voltage at zero concentration of carbonate in the same supporting electrolyte was also recorded for the purpose of comparison. It was observed that the current, presumably from electro-oxidation of water to O_2 in this condition, was much smaller than those at non-zero carbonate concentrations.

In a subsequent experiment the current–potential curve was examined over a range of electrode rotation rate from 400 to 3600 rpm in 1.13 M carbonate. The results of this experiment (reported below in Figure 4) show that the disk current (I_D) was essentially independent of electrode rotation rate, suggesting that the diffusion of electro-active species ($CO_3^{2-} + HCO_3^-$) is not a rate-determining step in these solutions, and that the electro-oxidation of carbonate is under kinetic control.

The linear relationship between oxidation current and carbonate concentration (Figure 3) indicates that the order of the primary electrode reaction (reaction I) is one, in other words, the reaction order for carbonate concentration is one. However, as written in the reaction I or VIII, the reaction order for carbonate ion should be two. This contradiction can be rationalized through a reaction mechanism that involves a unimolecular rate controlling step, such as the charge transfer to CO_3^{2-} followed by the fast dimerization of the subsequent carbonate radical to form $C_2O_6^{2-}$ [5, 10]. As mentioned in the "Introduction" of this paper, such details of the reaction mechanism will not be pursued here. A reaction order of one for carbonate ion will be used in the kinetic calculations of the following section.

The intercept of each line in Figure 3 can be approximated to the background current (I_B) from water electro-oxidation to O_2 (reaction IV) at the corresponding electrode potential. The slope of each line and the net disk current (I'_D) for carbonate oxidation at each electrode potential, obtained by subtracting the corresponding background current from the measured current (ie. $I'_D = I_D - I_B$), are used in the following theoretical treatment. During the electro-oxidation of carbonate on the disk electrode, the ring electrode is controlled at a potential (i.e.,

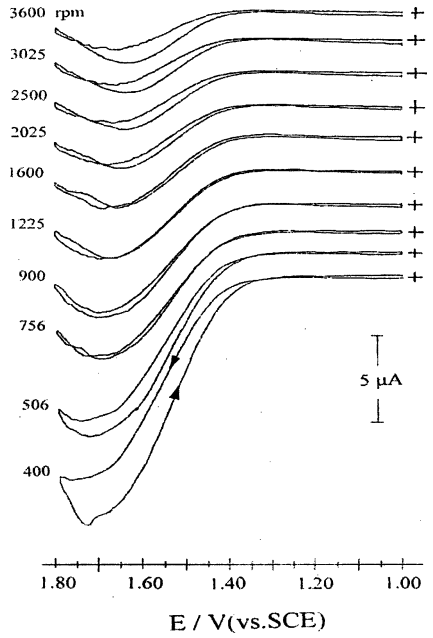

Fig. 4. Platinum ring currents vs disk potential at various rotation rates as marked at the left-side of the curves. During the recording, the platinum disk electrode was cycled from 1.00 to 1.80 V and at the same time, the ring potential was fixed at 1.01 V. The solution (as in Figure 2, pH 10.75) contains 1.13 M of (Na_2CO_3 + $NaHCO_3$). Potential scan rate: 50 mV s^{-1}.

1.01 V) to oxidize H_2O_2 which comes from the hydrolysis of percarbonate (reaction II) produced on the disk. Figure 4 shows the ring currents at a ring potential of 1.00 V, recorded when the disk was scanned from 1.00 to 1.80 V at various rotation rates in a solution containing 1.13 M total carbonate ($CO_3^{2-} + HCO_3^-$). The direction of the ring current (anodic direction) suggests that the current is not from the reduction of percarbonate, but from the oxidation of H_2O_2. In Figure 4, the ring current decreases with increasing rotation rate. Since the primary disk current is independent of rotation rate, the decreasing ring current provides information on the rate of percarbonate hydrolysis to H_2O_2 in reaction II [26–31]. A quantitative treatment of these data will be given later in this paper.

When the disk potential is more positive than about 1.7 V, the ring currents in Figure 4 decrease in the magnitude, due to the blocking-effect of gas (O_2) bubbles from the background reaction V. This blocking-effect of O_2 is seen in the noise on the current–potential curves (Figure 2). In the potential range of 1.40–1.60 V, no significant gas bubbles were observed on the electrode surface, and this range is used for quantitative treatment of carbonate electro-oxidation kinetics.

The stabilizer (Na_2SiO_3 + DTPA + $MgSO_4$) was used in our pulp brightening solution to suppress the decomposition of H_2O_2 [3]. This mixture of pulp brightening additives was also found necessary in the present tests to prevent both disk and ring current noise, without affecting the magnitude of the currents. The stabilizer appears only to increase the overpotential of background H_2O oxidation to O_2 and not to change the electrochemical behavior of carbonate oxidation. In any case the low concentrations of the stabilizer species impose a mass transport limiting current density for their possible reaction far below the current density of the primary anode reaction I.

3.2. *A proposed model for carbonate electro-oxidation kinetics*

For the electro-oxidation of carbonate in aqueous solutions [1–20], the overall reactions on a rotating platinum ring-disk electrode can be summarized as follows:

$$H_2CO_3 \overset{K_{a1}}{\longleftrightarrow} HCO_3^- + H^+ \quad \text{(Near disk electrode surface)} \qquad \text{(VI)}$$

$$HCO_3^- \overset{K_{a2}}{\longleftrightarrow} CO_3^{2-} + H^+ \quad \text{(Near disk electrode surface)} \qquad \text{(VII)}$$

$$2CO_3^{2-} \xrightarrow{k_1} C_2O_6^{2-} + 2e^- \quad \text{(On disk electrode)} \qquad \text{(VIII)}$$

$$C_2O_6^{2-} + 2H_2O \xrightarrow{k_h} H_2O_2 + 2HCO_3^- \quad \text{(On disk electrode surface)} \qquad \text{(IX)}$$

$$C_2O_6^{2-} \xrightarrow{r_1\omega^{1/2}} C_2O_6^{2-} \quad \text{(Diffusion from disk surface to the bulk solution)} \qquad \text{(X)}$$

$$C_2O_6^{2-} + 2H_2O \xrightarrow{W_1\omega^{-1/2}k_{hb}} H_2O_2 + 2HCO_3^- \quad \text{(Inside the diffusion layer)} \qquad \text{(XI)}$$

$$H_2O_2 \xrightarrow{k_2} O_2 + 2H^+ + 2e^- \quad \text{(On disk electrode)} \qquad \text{(XII)}$$

$$H_2O_2 \xrightarrow{k_d} 1/2\,O_2 + H_2O \quad \text{(On disk electrode surface)} \qquad \text{(XIII)}$$

$$H_2O_2 \xrightarrow{r_2\omega^{1/2}} H_2O_2(\text{ Diffusion from near the disk surface and detected by the ring electrode on which the oxidation is as reaction (XII))} \qquad \text{(XIV)}$$

$$H_2O_2 \xrightarrow{W_2\omega^{-1/2}k_{db}} 1/2\,O_2 + H_2O \quad \text{(Inside the diffusion layer)} \qquad \text{(XV)}$$

The equilibrium reactions (VI) and (VII) with reaction equilibrium constant K_{a1} and K_{a2} are assumed fast so that their kinetics are not considered here. Equation (VIII) represents the electro-oxidation of carbonate to percarbonate on the platinum rotating disk electrode, with a potential-dependent (pseudo) first-order rate constant k_1. Equation (IX) represents the hydrolysis of percarbonate to hydrogen peroxide on the electrode surface with a pseudo first-order rate constant k_h. The diffusion rate constant of Equation (X) can be considered as $r_1\omega^{1/2}$, where $r_1 = 0.201(D_{C_2O_6}^{2-})^{2/3}\nu^{-1/6}(D_{C_2O_6}^{2-})$ is the diffusion coefficient of percarbonate, ν is the kinematic viscosity of aqueous solutions [32], and ω is the electrode rotation rate. During the diffusion process, the $C_2O_6^{2-}$ can also react inside the diffusion layer as expressed as Equation (XI) with a rate constant of $w_1\omega^{-1/2}k_{hb}$, where $w_1\omega^{-1/2}$ is the diffusion layer thickness for $C_2O_6^{2-}$ ($w_1 = 4.98(D_{C_2O_6})^{1/3}\nu^{1/6}$) and k_{hb} is the bulk solution dissociation constant Equation (XII) represents the electro-oxidation of hydrogen peroxide from the reaction (IX), and k_2 is its potential dependent rate constant. Reaction (XIII) is the disproportionation of H_2O_2 occurring on the electrode surface with a rate constant of k_d. Another sink for H_2O_2, described by Equation (XIV), is diffusion into the bulk solution, which subsequently produces the ring currents of Figure 4. The diffusion rate constant, $r_2\omega^{1/2}$, is defined

in the same way as that of diffusion process (X), where $r_2 = 0.201(D_{H_2O_2})^{2/3}v^{-1/6}$($D_{H_2O_2}$is the diffusion coefficient of H_2O_2). The disproportionation of H_2O_2 inside the diffusion layer is expressed as Equation (XV) with a rate constant of $w_2\omega^{-1/2}k_{db}$, where $w_2\omega^{-1/2}$ is the diffusion layer thickness for $H_2O_2 w_2 = 4.98(D_{H_2O_2})^{1/3}v^{1/6})$, and k_{hb} is the bulk solution dissociation constant of H_2O_2.

Assuming steady-state in the diffusion layer. The material balance for $C_2O_6^{2-}$ is:

$$k_1[CO_3^{2-}] = k_h[C_2O_6^{2-}] + r_1\omega^{-1/2}[C_2O_6^{2-}] + w_1\omega^{1/2}k_{hb}[C_2O_6^{2-}] \quad (1)$$

where $[CO_3^{2-}]$ is expressed as Equation (2) according to reactions (VI) and (VII):

$$[CO_3^{2-}] = C_{CO_3}K_{a1}K_{a2}/([H^+]^2 + K_{a1}[H]^+ + K_{a1}K_{a2}) \quad (2)$$

Therefore, Equation (1) becomes Equation (3):

$$k_1 C_{CO_3}K_{a1}K_{a2}/([H^+]^2 + K_{a1}[H^+] + K_{a1}K_{a2}) = k_h[C_2O_6^{2-}] + r_1\omega^{1/2}[C_2O_6^{2-}] + w_1\omega^{-1/2}k_{hb}[C_2O_6^{2-}] \quad (3)$$

Note that the reaction order for CO_3^{2-} is 1 as proven in Figure 2.

Similarly the material balance for H_2O_2 in the diffusion layer is

$$k_h[C_2O_6^{2-}] + w_1\omega^{-1/2}k_{hb}[C_2O_6^{2-}] = k_2[H_2O_2] + k_d[H_2O_2] + r_2\omega^{1/2}[H_2O_2] + w_2\omega^{-1/2}k_{db}[H_2O_2]. \quad (4)$$

From Equation (3), the steady concentration of $C_2O_6^{2-}$ in the diffusion layer can be obtained, that is:

$$[C_2O_6^{2-}] = k_1(C_{CO_3}K_{a1}K_{a2}/([H^+]^2 + K_{a1}[H^+] + K_{a1}K_{a2}))/(k_h + r_1\omega^{1/2} + w_1\omega^{-1/2}k_{hb}), \quad (5)$$

and the corresponding steady concentration of H_2O_2 is derived from Equations (4) and (5):

$$[H_2O_2] = (K_h + w_1\omega^{-1/2}k_{hb})k_1(C_{CO_3}K_{a1}K_{a2}/([H^+]^2 + K_{a1}[H^+] + K_{a1}K_{a2}))/((k_h + r_1\omega^{1/2} + w_1\omega^{-1/2}k_{hb})(k_2 + k_d + r_2\omega^{1/2} + w_2\omega^{-1/2}k_{db})) \quad (6)$$

Assuming that CO_3^{2-} and H_2O_2 are the electro-active species the disk current is expressed as:

$$I_D' = n_1FAk_1(C_{CO_3}K_{a1}K_{a2}/([H^+]^2 + K_{a1}[H^+] + K_{a1}K_{a2})) + n_2FAk_2[H_2O_2] \quad (7)$$

where $n_1(=2)$ and $n_2(=2)$ are the electron stoichiometry coefficients for reactions (VIII) and (XII), respectively, F is Faraday's constant and A is the disk electrode area (cm^2). The replacement of $[H_2O_2]$ in Equation (7) by Equation (6) gives an Equation (8):

$$I_D' = 2FAk_1(C_{CO_3}K_{a1}K_{a2}/([H^+]^2 + K_{a1}[H^+] + K_{a1}K_{a2}))\{1 + k_2(k_h + w_1\omega^{-1/2}k_{hb})/((k_h + r_1\omega^{1/2} + w_1\omega^{-1/2}k_{hb})(k_2 + k_d + r_2\omega^{1/2} + w_2\omega^{-1/2}k_{db}))\}. \quad (8)$$

According to rotating ring disk theory [27, 28], the ring current for peroxide oxidation can be described as Equation (9):

$$I_R = n_2FAr_2\omega^{1/2}[H_2O_2]N^\circ \quad (9)$$

where N° is the ring collection efficiency. Substituting Equation (6) into Equation (9) gives Equation (10):

$$I_R = 2FAr_2\omega^{1/2}k_1(k_h + w_1\omega^{-1/2}k_{hb})N^\circ C_{CO_3}K_{a1}K_{a2}/([H^+]^2 + K_{a1}[H^+] + K_{a1}K_{a2})/((k_h + r_1\omega^{1/2}w_1\omega^{-1/2}k_{hb})(k_2 + k_d + r_2\omega^{1/2} + w_2\omega^{-1/2}k_{db})). \quad (10)$$

The combination of Equations (8) and (10) leads to an expression (Equation (11)) from which the kinetics rate constants are evaluated:

$$(I_D'/I_R)N^\circ = \{1/[r_2\omega^{1/2}(k_h + w_1\omega^{-1/2}k_{hb})]\} * [(k_h + r_1\omega^{1/2} + w_1\omega^{-1/2}k_{hb})(k_2 + k_d + r_2\omega^{1/2} + w_2\omega^{-1/2}k_{db}) + k_2(k_h + w_1\omega^{-1/2}k_{hb})] \quad (11)$$

As an approximation, it is assumed that $D_{C_2O_6}^{2-} = D_{H_2O_2} = 1.0 \times 10^{-5}$ cm^2 s^{-1} at room temperature (25 °C) [33], $w_1 = w_2 = 5.13 \times 10^{-2}$ cm $s^{-1/2}$, and $r_1 = r_2 = 2.0 \times 10^{-4}$ cm $s^{-1/2}$. Based on the experimental data, Equation (11) can be employed to estimate the reaction rate constants.

In the measurements (Figures 2 and 4), $(I_D'/I_R)N^\circ$ in Equation (11) can be obtained at various electrode rotation rates, then the plots of $(I_D'/I_R)N^\circ$ vs $\omega^{1/2}$ at various potentials allows the estimation of the rate constants, such as k_h, k_2, k_d, k_{hb}, and k_{db}. The data from Figures 2 and 4 were simulated according to Equation (11) as shown in Figure 5. From Figure 5, it can be seen that the simulated lines are in good agreement with the values obtained by experiment.

In the simulation, the values of k_d and k_{db} were adopted from references as, respectively $(1.6 \pm 0.3) \times 10^{-4}$ cm s^{-1} [31], and $(6.0 \pm 1.0) \times 10^{-5}$ s^{-1} [34]. The other two potential-independent constants obtained by this simulation are: $k_h = (2.0 \pm 0.3) \times 10^{-4}$ cm s^{-1}, and $k_{hb} = (1.1 \pm 0.2) \times 10^{-2}$ s^{-1}, respectively. For the H_2O_2 oxidation rate constant, k_2, which is potential-dependent, the simulated values are listed in Table 1.

The potential dependent constant k_2 for H_2O_2 electrooxidation on the platinum surface (reaction (VII)) is shown in Figure 6. The linear relationship between the $\log(k_2)$ and electrode potential suggests that the behavior could be expressed as a Tafel form:

$$\log(k_2) = \log(k_2^\circ) + (\alpha_2 n_{\alpha 2}F/2.303RT)(E - E^{o(H_2O_2/O_2)}) \quad (12)$$

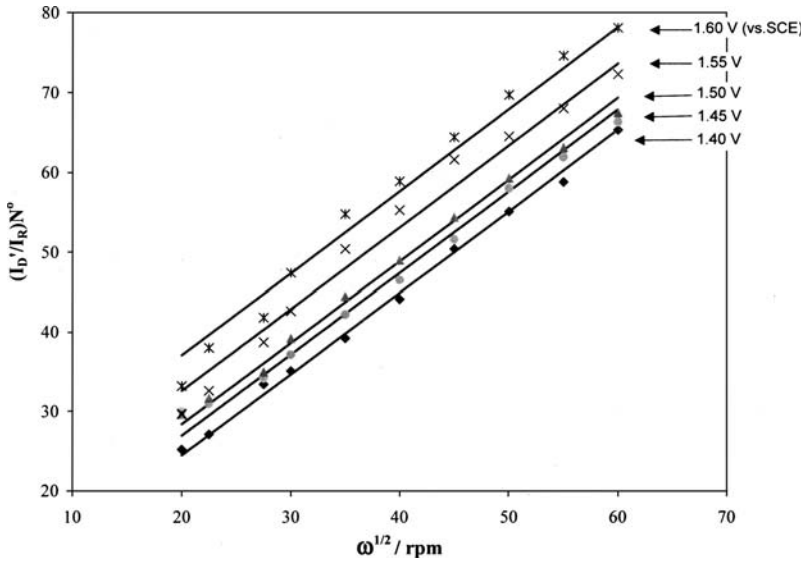

Fig. 5. Plots of $(I'_D/I_R)N^\circ$ vs square root of electrode rotating rate ($\omega^{1/2}$) at various disk potentials as marked at the right-side of the plots. The data are from Figure 4. The solid lines are those simulated, and the points are those experimentally measured.

Table 1. H_2O_2 oxidation kinetic constant k_2 at various electrode potentials. 25° *C*, pH 10.75

Electrode potentials V (vs SCE)	1.40	1.45	1.50	1.55	1.60
$k_2 10^4$cm s^{-1}	9.9 ± 0.3	15.0 ± 0.4	18.0 ± 0.5	26.0 ± 0.8	35.0 ± 0.9

where k_2° is a standard rate constant at equilibrium potential $E^{\circ(H_2O_2/O_2)}$ of the H_2O_2/O_2 redox couple ($E^o = -0.19$ V at pH 10.75 at 25 °C [32]), $\alpha_2 n_{\alpha 2}$ is the product of electron transfer coefficient (α_2) and controlling-step electron transfer, number ($n_{\alpha 2}$) for the corresponding process, and E is the electrode potential. The plot of $\log(k_2)$ vs E in Figure 6 was used to estimate the values of k_2^0 and $\alpha_2 n_{\alpha 2}$. The value of α_2 is found to be 0.16 (assuming $n_{\alpha 2} = 1$) while k_2° is $(5.6 \pm 0.) \times 10^{-8}$ cm s^{-1} On the other hand, the plot can be employed to roughly estimate the rate constant at any chosen potential in the experimental range.

The rate constant k_1 was obtained from the experimental data in Figure 3 and Equation (8). In Equation (8), the term of $k_2(k_h + w_1\omega^{-1/2}k_{hb})/((k_h + r_1\omega^{1/2} + w_1\omega^{-1/2}k_{hb})(k_2 + k_d + r_2\omega^{1/2} + w_2\omega^{-1/2}k_{hb}))$ inside the parentheses is much smaller than 1, therefore the equation can be simplified as:

$$I'_D = 2FAk_1C_{co_3}K_{a1}K_{a2}/([H^+]^2 + K_{a1}[H^+] + K_{a1}K_{a2}) \quad (13)$$

that is, a linear relationship between the disk current and concentration of carbonate. This linear relationship is proven by the data of Figure 3 if the background current is assumed to be a constant value at different concentrations of carbonate. The slope of each line in Figure 3 gives a value of $2FAk_1K_{a1}K_{a2}/([H^+]^2 + K_{a1}[H^+] + K_{a1}K_{a2})$, from which k_1 was evaluated using the solution pH (= 10.75) and the known values of the acidic

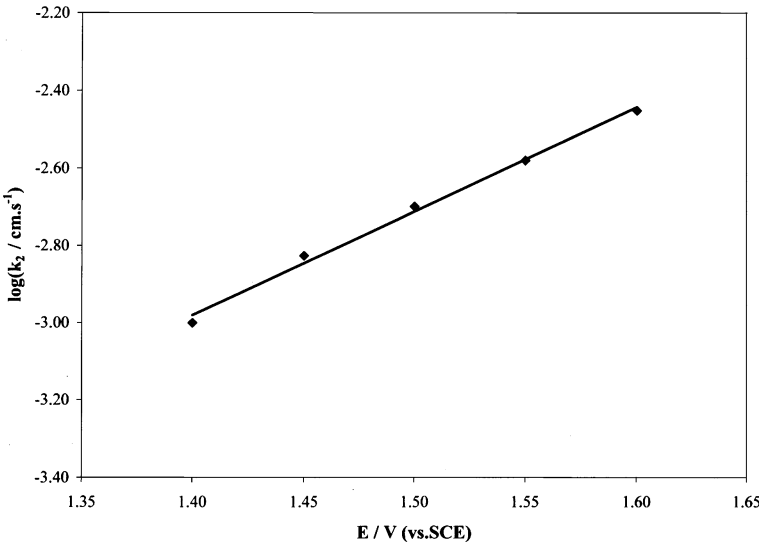

Fig. 6. Potential dependence of rate constant (k_2) for H_2O_2 electrooxidation.

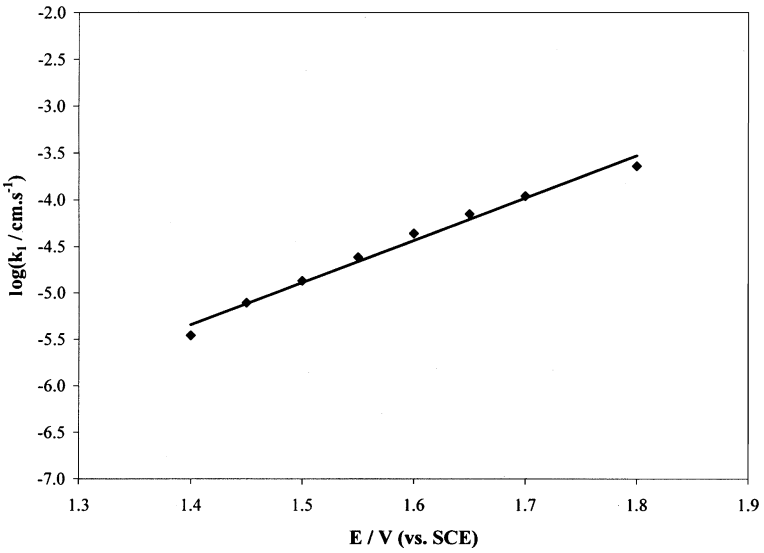

Fig. 7. Potential dependence of logarithmic rate constant (k_1) for carbonate electro-oxidation.

Table 2. Simulated reaction constants

Reaction I		Reaction II		Reaction III		Reaction IV	
k_1^o	$\alpha_1 n_{\alpha 1}$	k_h	k_{hb}	k_2^o	$\alpha_2 n_{\alpha 2}$	k_d^*	k_{db}^{**}
10^{11}cm s^{-1}		10^4 cm s^{-1}	10^2 s^{-1}	10^8cm s^{-1}		10^4 cm s^{-1}	10^5 s^{-1}
1.430 ± 0.1	0.27	2.0 ± 0.3	1.1 ± 0.2	5.6 ± 0.5	0.16	1.6 ± 0.3	6.0 ± 1.0

* From Reference [31]
** From Reference [34]

equilibrium constants $K_{a1}(4.2 \times 10^{-7}\,\text{mol dm}^{-3})$ and $K_{a2}(5.6 \times 10^{-11}\,\text{mol dm}^{-3})$ [32].

Figure 7 displays a relationship between $\log(k_1)$ and electrode potential (E). Assuming Tafel kinetics the potential dependence of k_1 may be expressed as equation (14):

$$1\log(k_1) = 1\log(k_1^\circ) + (\alpha_1 n_{\alpha 1} F/2.3RT)(E - E^{\circ(C_2O_6/CO_3)}) \quad (14)$$

from which a value of electron transfer coefficient (α_1) for carbon electro-oxidation was obtained, that is 0.27 (assuming $n_{\alpha 1} = 1$). If the standard equilibrium electrode potential ($E^{\circ(C_2O_6/CO_3)}$) of the couple $CO_3^{2-}/C_2O_6^{2-}$ is presumed to be 0.21 V at 25 °C and pH 10.75 [7], and the acidic association constants of H_2CO_3 are taken as above, the standard rate constant for carbonate oxidation at E^o (0.21 V) according to Figure 6 is 1.43×10^{-11} cm s^{-1}.

4. Conclusion

The kinetic model developed here for carbonate electro-oxidation on platinum gives a satisfactory fit to the experimental results. For carbonate oxidation near/in the potential range of H_2O oxidation (i.e. > 1.7 V), the measurement accuracy of the rotating ring-disk electrode is limited by the background reaction that creates O_2 bubbles on the electrode surface (blocking-effect). Nevertheless, the data can be used to model the carbonate/ percarbonate system by selecting values in the potential range 1.40–160 V. Rate constants for the reactions in the proposed sequence were obtained from these data and are summarized in Table 2.

The anode current efficiency $(CE)_{anode}$ for electro-oxidation of carbonate to percarbonate at various CO_3^{2-} concentrations and electrode potentials may be estimated from the data in Figure 3, as

$$(CE)_{anode} = (I_D - I_B)/I_D$$

and this value ranges up to about 80% at an anode potential of 2.0 V.

The reaction parameters found here are useful as a starting point to describe the electro-oxidation of carbonate and the electrochemical generation of peroxide for electro-brightening of pulp [3, 34]. However substantially more data, over practical ranges of composition and temperature, are needed for an engineering model of this system.

Acknowledgment

We are indebted to the Mechanical and Chemimechanical Pulps Network (One of fifteen Networks of Centres of Excellence supported by the Government of Canada), PAPRICAN, the University British Columbia and the UBC Pulp and Paper Centre. Discussion with Dr. Jinru Wang about computer simulation are gratefully acknowledged.

References

1. N.E. Khomutov and N.A. Meshcherova, *Deposited Doc.*, VINITI 5137–81, (1981) 10 (Chemical Abstracts, 98, 24533a).
2. O.G. Malin, N.E. Khomutov and V.V. Tsodikov, *Zh. Prikl. Khim.* **59**(6) (1986) 1338.
3. J. Jung, *"Electro-brightening of Mechanical Pulp"*. M.A.Sc. Thesis. Department of Chemical Engineering. The University of British Columbia, (1999).
4. E.J. Constam and A. Hansen, *Zeit. Fur Elektrochemie* **7** (1896) 18.
5. N.E. Khomitov, M.F. Sorokina and O.V. Shelud'ko, *Tr. Mosk. Khim. – Tekhnol. Inst.* **44** (1963) 63.
6. I.F. Franchuk and A.I. Brodskii, *Doklady Akad. Nauk S. S. S. R.* **118** (1958) 128.
7. A.Y. Prokopchikas and A.I. Vashkyalis. *in* I.I. Chernyayev (Ed), Chemistry of Peroxide Compounds, (Publishing House of the Academy of Science of the USSR, Moscow, 1963), pp. 228–236.
8. A. Prokopcikas and A. Vaskelis, *Lietuvos TSR Mokslu. Akad. Darbai (ser B)* **1** (1963) 61.
9. A. Vaskelis and A. Prokopcikas, *Lietuvos TSR Mokslu. Akad. Darbai (Ser B)* **2** (1963) 75.
10. N.E. Khomitov and L.S. Filatova, *Tr. Mosk. Khim. – Tekhnol. Inst.* **60** (1969) 65.
11. N.E. Khomitov and L.S. Filatova, *Tr. Mosk. Khim. Tekhnol. Inst.* **62** (1969) 211.
12. P.M. Van der Wiel, L.J.J. Janssen and J.G. Hoogland, *Electrochim. Acta* **16**(8) (1971) 1217.
13. P.M. Van der Wiel, L.J.J. Janssen and J.G. Hoogland, *Electrochim. Acta* **16**(8) (1971) 1227.
14. A.A. Krimshtein, L.V. Bondarenko, Z.M. Udaleeva and T.P. Firsova, *Tezisy Dokl. Vses. Soveshch. Khim. Neorg. Perekisnykh Soedin*, (1973) 43.
15. N.T. Toroptseva, L.S. Filatova and N.E. Khomutov, *Tezisy Dokl. Vses. Soveshch. Khim. Neorg. Perekisnykh Soedin*, (1973) 55.
16. L.S. Filatova, M.F. Sorokina, and N.E. Khomutov, *Tezisy Dokl. Vses. Soveshch. Khim. Neorg. Perekisnykh Soedin*, (1973) 57.
17. L.E. Voropaev, I.M. Zharskii, A.V. Kapitsa and V.N. Stanishevskii, *Khim. Khim. Tekhnol. (Minsk)* **20** (1985) 43.
18. N.T. Toroptseva, M.V. Raevskaya, Konobas Yu. I. and E.M. Sokolovskaya, *Vestn Mosk. Univ., (Ser 2): Khim* **28**(3) (1987) 263.
I9. N.T. Toroptseva and A.Y. Vaseva, *Zh. Prikl. Khim. (Leningrad)* **61**(2) (1988) 402.
20. K.N. Nikitin, N.A. Zakhodyakina, T.N. Skornyakova and A.V. Khitrova, *Izv. Vyssh. Uchebn. Zaved., Khim. Khim. Tekhnol.* **33**(5) (1990) 66.
21. Kirk-Othmer, 'Encyclopedia of Chemical Technology', 3rd ed., (Wiley, New york, 1982) pp. 9.
22. V.I. Kvlividze, T.P. Firsova and E.Y. Filatov, *Izv. Akad. Nauk. SSSR Ser. Khim.* **8** (1969) 1714.
23. V.I. Sakol, V.M. Bakulina, E.Y. Filatov and T.P. Firsova, *Zh. Neorg. Khim.* **13** (1968) 2347.
24. C.W. Jones. Application of Hydrogen Peroxide and Derivatives, *in* J.H. Clark (Ed), RSC Clean Technology Monographs, (Cambridge, UK, 1999), pp. 41–43.
25. M.A.A.F. Carrondo, W.P. Griffith, D.P. Jones and A.C. Skapski, *J. Chem. Soc., Dalton Trans.*, (1977) 2323.
26. A.J. Bard and L.R. Faulkner, *Electrochemical Methods, Fundamentals and Applications* (Wiley, New York, 1980).
27. J. Koutecky and V.G. Levich, *Zh. Fiz. Khim.* **32** (1958) 1565.
28. V.G. Levich, *Physicochemical Hydrodynamics* (Prentice Hall, Englewood Cliffs NJ, 1962), pp. 345.
29. W.J. Albery and M.L. Hitchman, *Ring-Disk Electrodes* (Clarendon Press, Oxford, 1971).
30. H.S. Wroblowa, Y.C. Pan and G. Razumney, *J. Electroanal. Chem.* **69** (1976) 196.
31. F. Van Den Brink, E. Barendrecht and W. Visscher, *J. Electrochem. Soc.* **127** (1980) 2003.
32. D.R. Lide, *Handbook of Chemistry and Physics* (CRC, New York, 1995–1996).
33. I.O. Zaytsev and G.G. Aseyev, *Properties of Aqueous Solutions of Electrolytes* (CRC Press, Boca Raton, FL, 1992).
34. H. Lee, A.H. Park and C. Oloman, *Tappi J.* **83**(8) (2000) 70.